

BLOC-3, a Protein Complex Containing the Hermansky-Pudlak Syndrome Gene Products HPS1 and HPS4*

Received for publication, February 5, 2003, and in revised form, May 15, 2003
Published, JBC Papers in Press, May 19, 2003, DOI 10.1074/jbc.M301294200

José A. Martina, Kengo Moriyama, and Juan S. Bonifacino‡

From the Cell Biology and Metabolism Branch, NICHD, National Institutes of Health, Bethesda, Maryland 20892

The Hermansky-Pudlak syndrome (HPS) is a genetic disorder characterized by defective lysosome-related organelles. HPS results from mutations in either one of six human genes named *HPS1* to *HPS6*, most of which encode proteins of unknown function. Here we report that the human HPS1 and HPS4 proteins are part of a complex named BLOC-3 (for biogenesis of lysosome-related organelles complex 3). Co-immunoprecipitation experiments demonstrated that epitope-tagged and endogenous HPS1 and HPS4 proteins assemble with each other *in vivo*. The HPS1-HPS4 complex is predominantly cytosolic, with a small amount being peripherally associated with membranes. Size exclusion chromatography and sedimentation velocity analyses of the cytosolic fraction indicate that HPS1 and HPS4 form a moderately asymmetric protein complex with a molecular mass of ~175 kDa. HPS4-deficient fibroblasts from *light ear* mice display normal distribution and trafficking of the lysosomal membrane protein, Lamp-2, in contrast to fibroblasts from AP-3-deficient *pearl* mice (HPS2), which exhibit increased trafficking of this lysosomal protein via the plasma membrane. Similarly, *light ear* fibroblasts display an apparently normal accumulation of Zn²⁺ in intracellular vesicles, unlike *pearl* fibroblasts, which exhibit a decreased intracellular Zn²⁺ storage. Taken together, these observations demonstrate that the HPS1 and HPS4 proteins are components of a cytosolic complex that is involved in the biogenesis of lysosome-related organelles by a mechanism distinct from that operated by AP-3 complex.

A group of specialized cytoplasmic organelles including melanosomes and platelet dense bodies are biogenetically related to lysosomes, and are hence referred to as “lysosome-related organelles” (LROs)¹ (1). Both LROs and lysosomes are formed from the *trans*-Golgi network and endosomes by pathways that share various common steps involving vesicle budding, maturation, translocation, targeting, fusion, and fission. The distinctive properties of LROs, however, require the existence of additional, LRO-specific events for their biogenesis.

* The costs of publication of this article were defrayed in part by the payment of page charges. This article must therefore be hereby marked “advertisement” in accordance with 18 U.S.C. Section 1734 solely to indicate this fact.

‡ To whom correspondence should be addressed: Cell Biology and Metabolism Branch, NICHD, Bldg. 18T, Rm. 101, National Institutes of Health, Bethesda, MD 20892. Tel.: 301-496-6368; Fax: 301-402-0078; E-mail: juan@helix.nih.gov.

¹ The abbreviations used are: LRO, lysosome-related organelles; HPS, Hermansky-Pudlak syndrome; HPS1, HPS type 1; HPS4, HPS type 4; Lamp-1, lysosome-associated membrane protein 1; Lamp-2, lysosome-associated membrane protein 2; BLOC-1, -2, and -3, biogenesis of lysosome-related organelles complex 1, 2, and 3; AP, adaptor protein; HA, hemagglutinin.

Insights into the molecular machinery involved in LRO biogenesis have been recently gained from the study of genetic disorders that affect multiple LROs in both humans and mice (1–3). In both species, defects in the biogenesis of melanosomes and platelet dense bodies lead to reduced pigmentation and prolonged bleeding, respectively. One of these disorders, known as Chediak-Higashi syndrome in humans and the *beige* mutation in mice, is caused by mutations in a gene encoding the protein, *LYST* (4). Another human disorder, Hermansky-Pudlak syndrome (HPS), results from mutations in either one of six genes designated *HPS1*–*HPS6* (5–9). Mutations in the orthologous genes have been identified in the mouse coat color mutants, *pale ear* (*HPS1* (10, 11)), *pearl* (*HPS2* (12)), *cocoa* (*HPS3* (13)), *light ear* (*HPS4* (8)), *ruby eye-2* (*HPS5* (9)), and *ruby eye* (*HPS6* (9)), which serve as animal models for the human disease. Other studies have led to the identification of additional genes mutated in other mouse models of HPS, including *mocha* (14), *gunmetal* (15), *buff* (16), *pallid* (17), *muted* (18), and *cappuccino* (19). Mutations in the orthologous genes, however, have not yet been reported in HPS patients. Finally, the genes mutated in other mouse HPS models, including *subtle gray*, *reduced pigmentation*, and *sandy*, remain to be identified. *HPS2/pearl* and *mocha* encode the β 3A (6, 12) and δ subunits (14), respectively, of the adaptor protein (AP) complex, AP-3. This complex is a known component of the protein trafficking machinery and is involved in the sorting of the transmembrane proteins tyrosinase (21–23) and the quail neuroretina clone 71 (QNR-71) protein (24) to melanosomes. *Gunmetal* encodes the α subunit of Rab geranylgeranyl transferase, an enzyme that adds geranylgeranyl groups to Rab GTP-binding proteins (15). Finally, *buff* codes for VPS33A (16), a component of the HOPS-C-Vps complex involved in protein transport to the yeast vacuole and mammalian lysosomes (25, 26).

Strikingly, all the other HPS genes cloned to date encode novel proteins with no recognizable homology or structural motifs. Some of these novel proteins have been recently shown to be components of oligomeric complexes. For example, the products of the *pallid*, *muted*, and *cappuccino* genes are subunits of a cytosolic complex named BLOC-1 (for biogenesis of lysosome-related organelles complex 1) (19, 27, 28), whereas HPS5 and HPS6 form another cytosolic complex named BLOC-2 (9).

Several lines of evidence support the possibility that other HPS gene products might also be components of multiprotein complexes. *HPS1/pale ear* encodes an 80-kDa cytosolic protein (5, 29, 30), which is absent from *light ear* (HPS4-deficient) mouse platelets (8). This is reminiscent of cells deficient in AP-3 (6, 31) or BLOC-1 (19, 27, 28), in which the absence of one subunit leads to the loss of other subunits of the corresponding complex. This is the result of quality control mechanisms that dispose of unassembled subunits of multiprotein complexes. Moreover, the *pale ear* and *light ear* mutants (8), or the double-

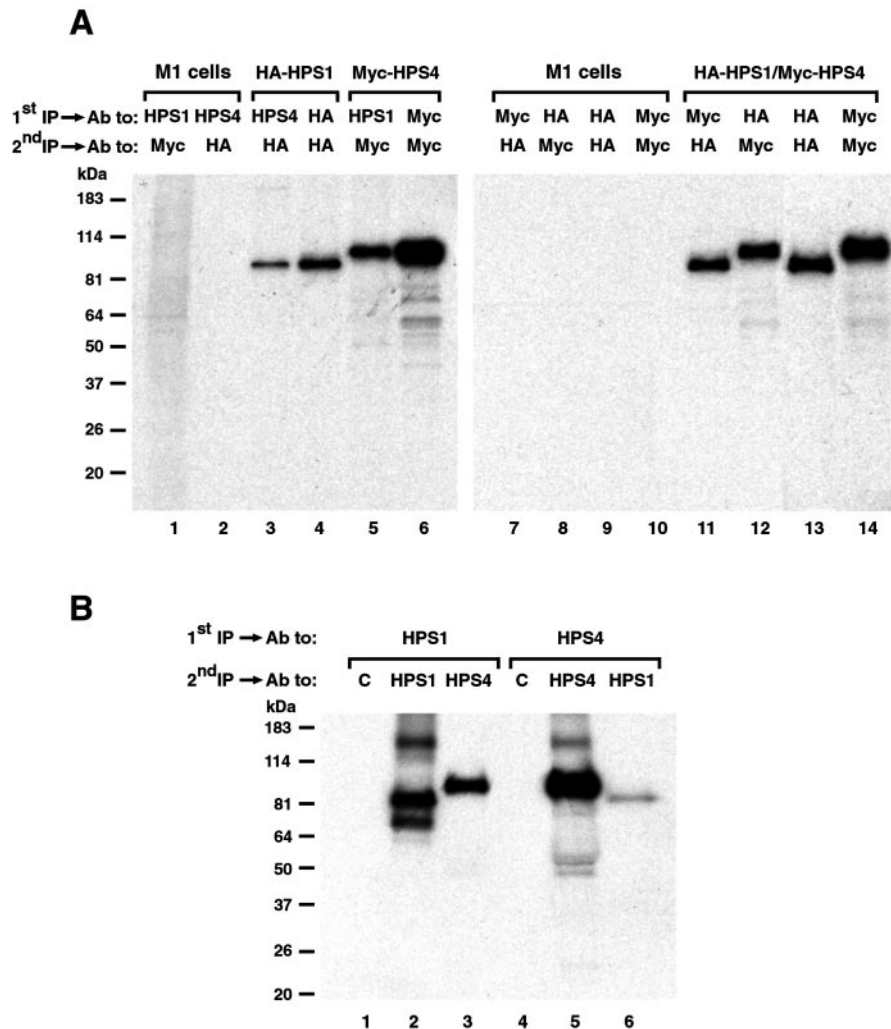


FIG. 1. Co-immunoprecipitation of HPS1 and HPS4. *A*, M1 fibroblast and stably transfected M1 clones expressing either HA₃-HPS1 (clone number 5) or Myc₃-HPS4 (clone number 26) or HA₃-HPS1 and Myc₃-HPS4 (clone number 42) were metabolically labeled with [³⁵S]methionine for 22 h and extracted with lysis buffer containing 0.5% (w/v) Triton X-100 (35). The extracts were then subjected to a first immunoprecipitation (1st IP) with affinity purified rabbit antibody to HPS1, rabbit antibody to HPS4, mouse monoclonal anti-HA or anti-Myc, as indicated. Washed immunoprecipitates were subsequently denatured by heating at 95 °C for 5 min in the presence of SDS and dithiothreitol, diluted with lysis buffer, and subjected to a recapture immunoprecipitation step (2nd IP) using either anti-HA or anti-Myc. The resulting immunoprecipitates were analyzed by SDS-PAGE on 4–20% gradients followed by fluorography. The signals shown in lanes 4, 6, and 14 correspond to 2% of the immunoprecipitated material; 5% of the immunoprecipitated material was loaded in lane 13, whereas 100% of the immunoprecipitated was loaded in lanes 3, 5, 11, and 12. *B*, whole cell extracts from metabolically labeled MNT-1 cells were subjected to immunoprecipitation-recapture analysis, as described in *A*, using either antibodies to the HPS1 or HPS4 proteins for the 1st IP and antibodies to an irrelevant protein (c), to the HPS1 or HPS4 proteins for the 2nd IP step. The ~175-kDa band present in lanes 2 and 5 seems to represent a nonspecific interaction since it was immunoprecipitated by the two different antibodies that were used. The identity of the ~70-kDa band in lane 2 is uncertain at this time, but may represent a minor degradation product of HPS1. The positions of molecular mass markers are indicated on the left.

homozygote mutant mice (32), show virtually identical phenotypes of reduced pigmentation limited to the ears and tail (8), indicating that HPS1 and HPS4 may interact physically and/or functionally.

Herein we demonstrate that HPS1 and HPS4 form a complex that we name BLOC-3. Both the endogenous and exogenously expressed, epitope-tagged forms of human HPS1 and HPS4 co-precipitate and co-migrate with each other on sedimentation velocity and gel filtration analyses. The sedimentation coefficient and size exclusion chromatographic properties of BLOC-3 differ from those of AP-3 and BLOC-1, consistent with the existence of multiple complexes involved in the biogenesis of LROs. BLOC-3 appears to be mostly cytosolic on subcellular fractionation, although a small fraction is peripherally associated with membranes. In contrast to AP-3-deficient cells (6, 22, 29, 33), *light ear* (HPS4-deficient) cells exhibit normal trafficking of lysosomal membrane proteins and normal storage of Zn²⁺ in intracellular vesicles. These observations indicate that

AP-3 and BLOC-3 mediate distinct steps in the biogenesis of LROs.

EXPERIMENTAL PROCEDURES

DNA Constructs—The constructs pCI-HA₃ and pCI-Myc₃ were generated by cloning of annealed primers containing three copies of the HA and Myc epitope tags into *Xho*I-*Hind*III and *Xho*I-*Eco*RI sites of the mammalian expression vector pCI-neo (Promega, Madison, WI), respectively. The epitope tagging at the amino terminus of HPS1 and HPS4 was performed through PCR amplification of the full-length human HPS1 (GenBank™/EMBL/DDBJ accession number NM_000195) and HPS4 (GenBank™/EMBL/DDBJ accession number NM_022081) cDNAs, followed by in-frame cloning into *Hind*III-*Eco*RI sites of the pCI-HA₃ (pCI-HA₃-HPS1) and *Eco*RI site of the pCI-Myc₃ (pCI-Myc₃-HPS4) vectors, respectively. The inserts of these two plasmids were also subcloned into *Xho*I-*Not*I sites of the vector pCDNA3.1-hygromycin (Invitrogen). Yeast two-hybrid constructs in the pGBKT7 (TRP1) and pGADT7 (LEU2) vectors (Clontech) were prepared by cloning of both HPS1 and HPS4 full-length cDNAs.

Antibodies—The peptide sequence GKAKQKLLKHGVNLL, corre-

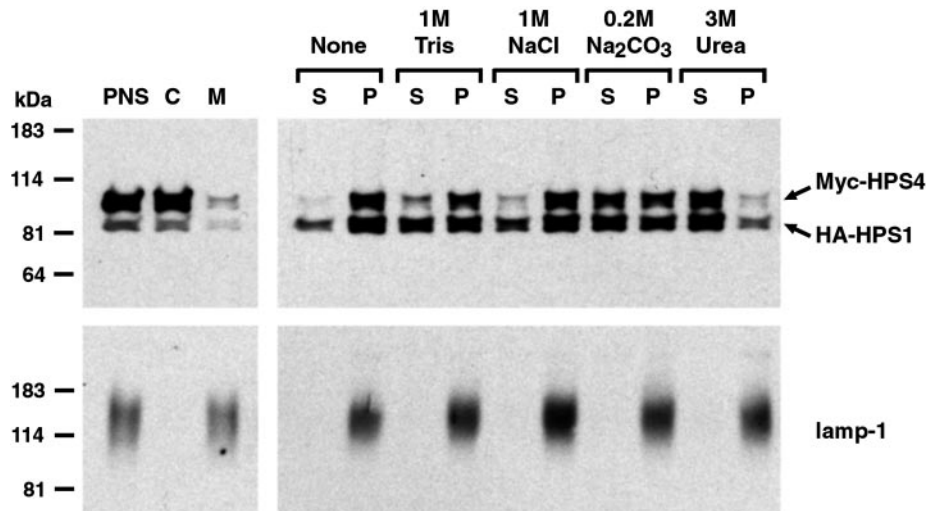


FIG. 2. HPS1 and HPS4 exist as soluble and membrane-associated forms. Cells stably expressing HA₃-HPS1 and Myc₃-HPS4 (clone number 42) were mechanically disrupted by successive passages through a 25-gauge needle in buffer A (25 mM HEPES, pH 7.4, 0.25 M sucrose, 1 mM EGTA, 0.5 mM MgCl₂, 1 mM dithiothreitol, and protease inhibitor mixtures). The material was subsequently centrifuged for 10 min at 800 × *g* to remove intact cells and nuclei. The post-nuclear supernatant (PNS) was then centrifuged at 120,000 × *g* for 2 h at 4 °C, to yield cytosol (C) and membrane (M) fractions. Subsequently, the membrane fraction was extracted for 45 min at 4 °C with 0.2× buffer A containing no additions (None) or the additives indicated in the figure. Supernatant (S) and pellet (P) fractions were prepared by ultracentrifugation. The presence of HA₃-HPS1 and Myc₃-HPS4 (upper panel) or Lamp-1 (lower panel), integral membrane protein control) in the various fractions was assessed by immunoblotting. The positions of molecular mass markers are indicated on the left.

sponding to residues 694–708 of human HPS4 (8) was used to generate a rabbit polyclonal antibody (AnaSpec Inc., San Jose, CA). The generation and purification of rabbit antibodies to AP3 β3A (34), HPS1 (29), and Pallidin (28) have been described previously. The following mouse monoclonal antibodies were also used: anti-HA (clone HA.11), anti-Myc (clone 9E10) (Covance, Richmond, CA), anti-γ1-adaptin AP1 (clone 100/3) (Sigma), anti-GGA3 (BD Transduction Laboratories, San Jose, CA). The monoclonal rat antibody to mouse Lamp-2 (clone ABL-93) was obtained from the Developmental Studies Hybridoma Bank (Iowa City, IA). Horseradish peroxidase-conjugated secondary antibodies for immunoblotting were from Amersham Biosciences. Alexa 488-conjugated goat anti-rat IgG, Alexa 488-conjugated goat anti-rabbit IgG, and Alexa 568-conjugated goat anti-mouse IgG were purchased from Molecular Probes (Eugene, OR).

Cell Culture and Transfection—The generation of cell lines derived from mouse skin fibroblasts and culture conditions for these and other cell lines have been described previously (29). Human M1 fibroblasts were stably transfected with either pCI-HA₃-HPS1 or pCI-Myc₃-HPS4 or with both pCI-HA₃-HPS1 and pCDNA-Hygro-Myc₃-HPS4 using the FuGENE 6 reagent (Roche Diagnostics). G418-resistant clones expressing HA₃-HPS1 (clone number 5) or Myc₃-HPS4 (clone number 36) were selected using 600 μg/ml G418. The clone expressing HA₃-HPS1 and Myc₃-HPS4 (clone number 42) was selected using 600 μg/ml G418 and 50 μg/ml hygromycin B.

Sedimentation Velocity Analysis and Size Exclusion Chromatography—Sedimentation velocity analysis was performed by ultracentrifugation on linear 2–15% (w/v) sucrose gradients (12 ml) prepared in buffer B (25 mM HEPES, pH 7.4, 150 mM NaCl, 1 mM EGTA, 1 mM dithiothreitol, 0.5 mM MgCl₂, and protease inhibitor mixture). Cytosol (350 μl) from cells either stably (clone number 42) or transiently expressing HA₃-HPS1 and Myc₃-HPS4, prepared in buffer B as described (36), was layered on top of a linear sucrose gradient and centrifuged in a SW41 rotor (Beckman Coulter Inc., Fullerton, CA) at 39,000 rpm for 17 h at 4 °C. Eighteen 0.65-ml fractions were collected from the bottom of the tube and analyzed by immunoprecipitation and immunoblotting. The following protein standards from Amersham Biosciences were used (Svedberg coefficients in parentheses): chicken ovalbumin (3.6 S), bovine serum albumin (4.6 S), rabbit aldolase (7.3 S), and bovine catalase (11.3 S).

For size exclusion chromatography analysis, 100 μl of cytosol from cells stably expressing HA₃-HPS1 and Myc₃-HPS4 (clone number 42) prepared in buffer B was applied to a calibrated Superdex 200 HR 10/30 column (Amersham Biosciences) equilibrated and eluted at 4 °C with buffer B at a flow rate of 0.3 ml/min. Fractions (0.4 ml) were collected and analyzed by immunoprecipitation and immunoblotting. Column calibration was performed using the following protein standards from Amersham Biosciences (Stokes radii in parentheses): bovine thyroglob-

ulin (85 Å), horse ferritin (61 Å), rabbit aldolase (48.1 Å), bovine serum albumin (35.5 Å), and chicken ovalbumin (30.5 Å). Molecular mass and frictional ratio (*f*/*f*₀) values were calculated from Stokes radii and sedimentation coefficients assuming a partial specific volume of 0.72–0.75 cm³/g, as described (37).

Electrophoresis and Immunoblotting—SDS-PAGE and immunoblotting analysis were performed as described (36). Horseradish peroxidase-labeled antibodies were detected by using the Western lightning, chemiluminescence reagent plus (PerkinElmer Life Sciences).

Antibody Internalization and Fluorescence Microscopy—Fibroblasts grown on glass coverslips were incubated for 15 min at 37 °C in the presence of primary antibodies diluted in Dulbecco's modified Eagle's medium, 0.5% (w/v) bovine serum albumin, and 25 mM HEPES, pH 7.4. Subsequently, cells were washed for 5 min in ice-cold phosphate-buffered saline, fixed in 4% formaldehyde for 15 min, and then processed for immunofluorescence (20). Images were acquired on a Zeiss LSM 410 confocal microscope (Carl Zeiss Inc., Thornwood, NY). To detect intracellular zinc store sites, either fixed or unfixed cells were incubated for 1 h with 25 μM zincquin ethyl ester (Toronto Research Chemicals, Ontario, Canada) in Dulbecco's modified Eagle's medium containing 25 mM HEPES, pH 7.4, and 0.1% (w/v) bovine serum albumin. Stained samples were washed extensively with phosphate-buffered saline and mounted on glass slides using Fluoromount G (Southern Biotech, Birmingham, AL). Images were acquired on a Zeiss LSM 410 confocal microscope using a 413-nm laser.

General Biochemical Procedures—Metabolic labeling of cultured cells with [³⁵S]methionine, preparation of Triton X-100 extracts, preparation and ultracentrifugation of detergent-free extracts, salt extraction of microsomal membranes, and immunoprecipitation-recapture were performed as described (35, 36).

Yeast Culture, Transformation, and Two-hybrid Assays—The *Saccharomyces cerevisiae* strain AH109 (Clontech) was transformed by the lithium acetate procedure as described in the instructions for the MATCHMAKER two-hybrid kit (Clontech). For colony growth assays, AH109 transformants were resuspended in water to 0.1 A₆₀₀/ml, then 5 μl were spotted on plates lacking leucine and tryptophan, in the presence or absence of histidine, and incubated at 30 °C for 4–5 days.

RESULTS

Co-immunoprecipitation of HPS1 and HPS4—The possible association of HPS1 with HPS4 was investigated in M1 human fibroblasts stably transfected with HA₃-tagged HPS1 and/or Myc₃-tagged HPS4. The association of these proteins was analyzed by immunoprecipitation-recapture (38) using extracts of M1 clones metabolically labeled with [³⁵S]methionine (Fig. 1). In cells expressing only HA₃-HPS1, this protein could be de-

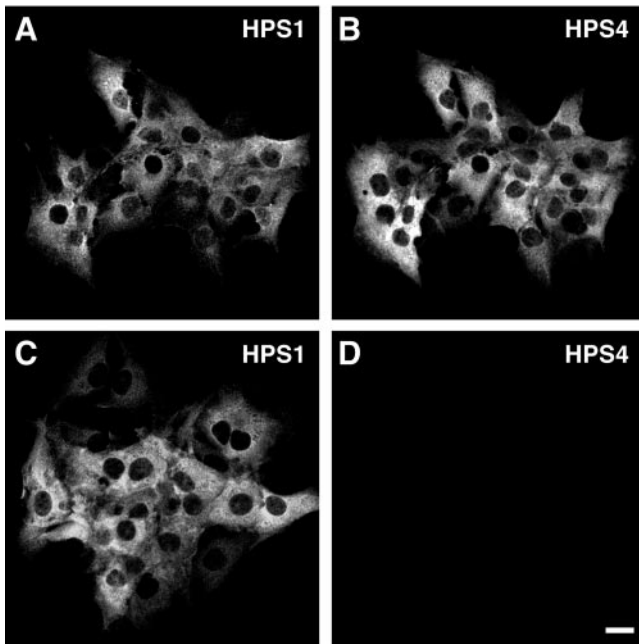


FIG. 3. Distribution of the HPS1-HPS4 complex in M1 cells stably expressing HA₃-HPS1 and Myc₃-HPS4. M1 fibroblasts stably expressing HA₃-HPS1 and Myc₃-HPS4 (clone number 42) were costained with mouse anti-HA antibody (A and C) to detect HA-HPS1 and a rabbit anti-serum (B) to detect HPS4 or the corresponding preimmune serum (D) followed by Alexa 568-conjugated anti-mouse IgG and Alexa 488-conjugated anti-rabbit IgG. Notice the diffuse cytoplasmic pattern of the HA₃-HPS1 and Myc₃-HPS4 proteins (A–C). Bar, 20 μ m.

ected as an ~88-kDa protein by the use of antibody to the HA epitope in both the immunoprecipitation and recapture steps (Fig. 1A, lane 4). This molecular mass is consistent with that previously reported for the endogenous protein (29, 30), accounting for the molecular mass of a triple HA epitope. Interestingly, use of an antibody to HPS4 in the immunoprecipitation step and an antibody to HA in the recapture step also resulted in the detection of the ~88-kDa HA₃-HPS1 (Fig. 1A, lane 3), consistent with the association of the endogenous HPS4 and the recombinant HA₃-HPS1 in these cells. In cells expressing only Myc₃-HPS4, immunoprecipitation and recapture with anti-Myc identified this protein as an ~98-kDa species (Fig. 1A, lane 6). This apparent molecular mass was larger than the ~78 kDa predicted from its amino acid sequence (8), even accounting for the contribution of a triple Myc epitope, indicating that HPS4 migrates anomalously on SDS-PAGE. Importantly, immunoprecipitation with anti-HPS1 followed by recapture with anti-Myc also yielded the ~98-kDa Myc₃-HPS4 (Fig. 1A, lane 5). This demonstrated that the endogenous HPS1 assembles with the transgenic Myc₃-HPS4. Similar experiments performed with cells expressing both HA₃-HPS1 and Myc₃-HPS4 demonstrated that these two epitope-tagged proteins also associate *in vivo* (Fig. 1, lanes 11–14).

The endogenous HPS1 and HPS4 were also found to interact with each other on immunoprecipitation-recapture analyses of untransfected MNT-1 (human melanoma) cells (Fig. 1B). This could be shown by immunoprecipitation with anti-HPS1 and recapture with anti-HPS4 (Fig. 1B, lane 3) or vice versa (Fig. 1B, lane 6). Taken together, these observations indicate that

FIG. 4. Sedimentation velocity analysis of the cytosolic HPS1-HPS4 complex. Cytosol from cells stably expressing HA₃-HPS1 and Myc₃-HPS4 (clone number 42) was fractionated by ultracentrifugation on a 2–15% (w/v) linear sucrose gradient as described under “Experimental Procedures.” A, samples representing 2% of the volume of each fraction were analyzed for the presence of HA₃-HPS1 and Myc₃-HPS4 by immunoblotting using both monoclonal anti-HA and anti-Myc antibodies. The presence of the HA₃-HPS1-Myc₃-HPS4 complex was assessed on samples (~40% of the volume of each fraction) either by immunoprecipitation using anti-HA and immunoblotting with anti-Myc antibodies (B) or immunoprecipitation using anti-Myc and immunoblotting with anti-HA antibodies (C). The sedimentation of three other endogenously expressed proteins was analyzed by immunoblotting using antibodies to γ 1 (AP-1) (D), GGA3 (E), and Pallidin (F). The positions of standard proteins (sedimentation coefficients given in Svedberg units) in the gradient are indicated on the top. The positions of molecular mass markers are indicated on the left.

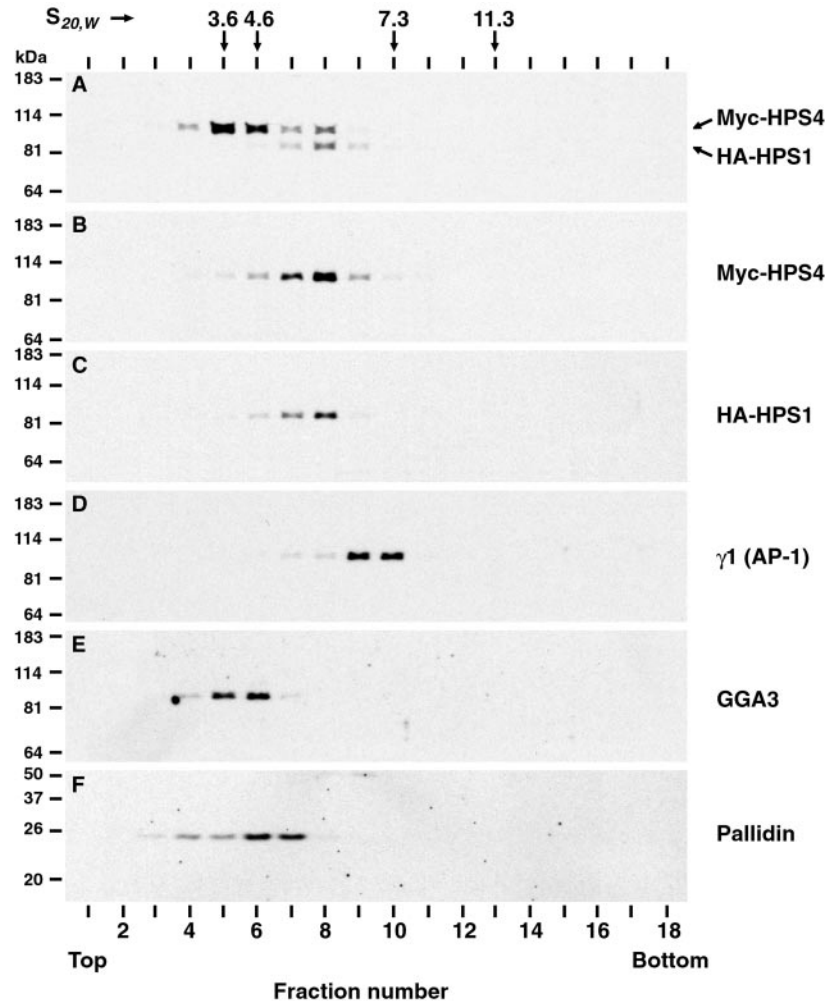
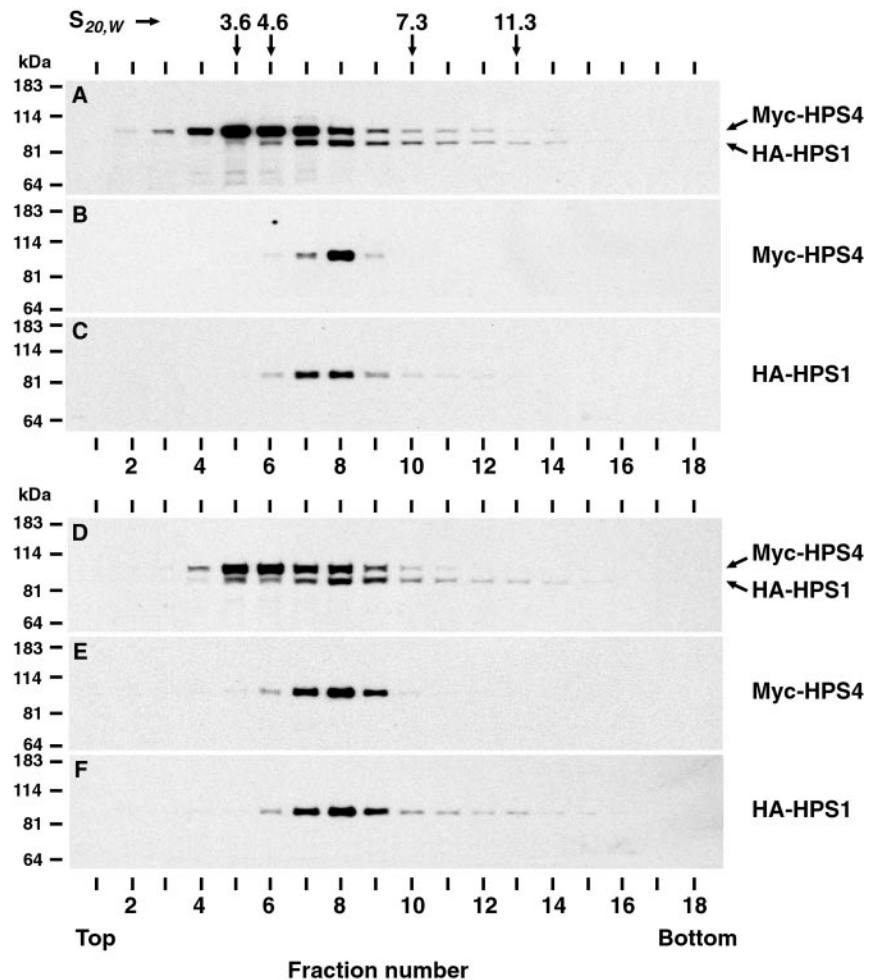


FIG. 5. Sedimentation velocity analysis of the cytosolic HPS1·HPS4 complex in human fibroblasts and melanocytes. Cytosol from M1 fibroblast (panels A–C) and MNT-1 (pigmented melanoma) cells (panels D–F) transiently expressing HA₃-HPS1 and Myc₃-HPS4 were fractionated by ultracentrifugation on 2–15% (w/v) linear sucrose gradients as described under “Experimental Procedures,” and the resulting fractions analyzed by immunoprecipitation and immunoblotting. Samples representing 2% of the volume of each fraction were analyzed for the presence of HA₃-HPS1 and Myc₃-HPS4 by immunoblotting using both monoclonal anti-HA and anti-Myc (A and D). The presence of the HA₃-HPS1·Myc₃-HPS4 complex was examined in samples of each fraction (50% of the volume) by immunoprecipitation using anti-HA and immunoblotting with anti-Myc (B and E). The same nitrocellulose membranes were used to detect the presence of the immunoprecipitated HA₃-HPS1 by immunoblotting with anti-HA antibody (C and F). The positions of standard proteins (sedimentation coefficients given in Svedberg units) are indicated on the top. The positions of the molecular mass markers are indicated on the left.



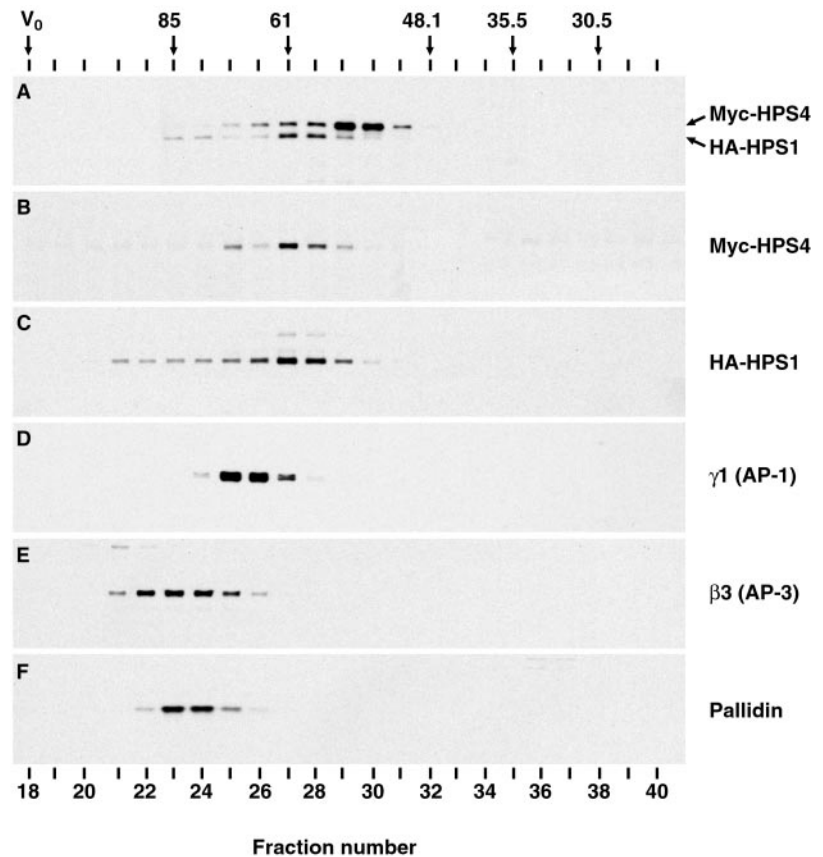
both the endogenous and epitope-tagged HPS1 and HPS4 associate with each other *in vivo*. We did not detect co-immunoprecipitation of HPS1 or HPS4 with Pallidin (data not shown), indicating that the HPS1·HPS4 complex is distinct from BLOC-1.

The HPS1·HPS4 Complex Is Mostly Cytosolic—To determine the extent to which the HPS1·HPS4 complex is associated with membranes, M1 cells stably expressing HA₃-HPS1 and Myc₃-HPS4 were homogenized in buffer A (20 mM HEPES, pH 7.4, 0.25 M sucrose, 1 mM EGTA, 0.5 mM MgCl₂, 1 mM dithiothreitol, and protease inhibitor mixture) and centrifuged for 10 min at 800 × *g*. The supernatant of this centrifugation (*i.e.* post-nuclear supernatant) was further centrifuged for 2 h at 120,000 × *g*, yielding cytosol (C) and membrane (M) fractions (Fig. 2, upper panel). Analysis by immunoblotting using anti-HA and anti-Myc showed that most of these proteins were in the cytosol with only a small fraction (less than 10%) being associated with membranes. These observations were consistent with similar analyses previously performed for endogenous HPS1 (29, 30), and also with immunofluorescence microscopy analyses that showed a predominantly cytosolic pattern for HA₃-HPS1 and Myc₃-HPS4 stably expressed in M1 cells (Fig. 3). The small fraction of membrane-associated HA₃-HPS1 and Myc₃-HPS4 could be extracted to various degrees with 1 M Tris-HCl (pH 7.4), 1 M NaCl, 0.2 M Na₂CO₃ (pH 11.3) or 3 M urea (Fig. 2, upper panel). These observations indicated that the association of HA₃-HPS1 and Myc₃-HPS4 with membranes is mostly peripheral. These properties of the HPS1·HPS4 complex are similar to those described before for the BLOC-1 complex (27, 28).

Hydrodynamic Properties of the HPS1·HPS4 Complex—The interaction of HPS1 with HPS4 was further characterized by conducting analyses of the sedimentation behavior of these proteins. To this end, extracts of M1 cells stably expressing both HA₃-HPS1 and Myc₃-HPS4 were subjected to sedimentation velocity analysis on sucrose gradients. Gradient fractions were assayed by immunoblotting with anti-HA and anti-Myc (Fig. 4). The distribution of Myc₃-HPS4 on the gradients exhibited two peaks corresponding to sedimentation coefficients of 3.8 S (fraction number 5) and 6.3 S (fraction number 8) (Fig. 4A). The second peak coincided with the HA₃-HPS1 peak (Fig. 4A). Immunoprecipitation with antibodies against one epitope followed by immunoblotting with antibodies to the other revealed a single peak at 6.3 S (Fig. 4, B and C). Therefore, the HPS1·HPS4 complex sediments as a 6.3 S species whereas the 3.8 S peak of Myc₃-HPS4 likely represents excess, unassembled protein. The sedimentation coefficient of the HPS1·HPS4 complex (6.3 S) was distinct from that of BLOC-1 as shown by immunoblotting with anti-Pallidin antibody (5.2 S, Fig. 4F and Refs. 27 and 28). This further confirmed that HPS1·HPS4 and BLOC-1 are distinct complexes.

Although mRNAs encoding HPS1 and HPS4 are expressed in most cells and tissues, the HPS1 or HPS4 mutant phenotype is manifested primarily in specialized cell types such as melanocytes and the platelet-precursor megakaryocytes. It is thus conceivable that the composition, and consequently the size, of the HPS1·HPS4 complex might be different in these specialized cell types. To address this issue, we co-expressed HA₃-HPS1 and Myc₃-HPS4 by transient transfection of M1 fibroblasts and MNT-1 melanocytes, and examined the sedimentation behav-

FIG. 6. Size exclusion analysis of the cytosolic HPS1·HPS4 complex. Cytosol from cells stably expressing HA₃-HPS1 and Myc₃-HPS4 was fractionated on a calibrated Superdex 200 HR column as described under "Experimental Procedures," and the resulting fractions were analyzed by immunoprecipitation and immunoblotting. *A*, samples representing 2% of the volume of each fraction were analyzed for the presence of HA₃-HPS1 and Myc₃-HPS4 by immunoblotting using both monoclonal anti-HA and anti-Myc antibodies. *B*, the presence of the complex HA₃-HPS1·Myc₃-HPS4 was examined in samples of each fraction (25% of the volume) by immunoprecipitation using anti-HA and immunoblotting with anti-Myc antibodies. *C*, the same nitrocellulose membrane was used to detect the presence of the immunoprecipitated HA₃-HPS1 by immunoblotting with anti-HA. The elution positions of three endogenously expressed proteins were analyzed by immunoblotting using antibodies to γ 1 (AP-1) (*D*), β 3A-adaptin (AP-3) (*E*), and Pallidin (*F*). The void volume (V_0) as well as the elution of standard proteins (Stokes radii given in Ångstroms) are indicated on the *top*.



ior of the complex as described above. The complex was found to migrate with an identical sedimentation coefficient of 6.3 S in both M1 and MNT-1 cells (Fig. 5, compare *B* and *E*). Hence, the distinct requirement for HPS1 and HPS4 in melanocytes is not likely because of a difference in the size, and presumably the composition, of the HPS1·HPS4 complex. However, we cannot rule out that endogenous levels of a melanocyte-specific protein putatively interacting with the HPS1·HPS4 complex could only affect the sedimentation properties of a small fraction of the recombinant complex.

The hydrodynamic properties of the HPS1·HPS4 complex were further characterized by size exclusion chromatography. An extract of M1 cells stably expressing HA₃-HPS1 and Myc₃-HPS4 was run on a Superdex 200 HR column and the eluted fractions analyzed by either immunoblotting or immunoprecipitation followed by immunoblotting (Fig. 6). Again, the distribution of total Myc₃-HPS4 showed two apparent peaks corresponding to Stokes radii of 65.2 and 55 Å (Fig. 6A). The first peak co-eluted with total HA₃-HPS1 (Fig. 6A) and thus corresponded to the HPS1·HPS4 complex (Fig. 6B). This was further confirmed by the elution of HA₃-HPS1 as identified by immunoprecipitation and immunoblotting (Fig. 6C). This gel filtration analysis also showed that the elution profile of the HPS1·HPS4 complex was distinct from those of the AP-3 complex detected by immunoblotting for β 3A-adaptin (Fig. 6E), and BLOC-1 detected by immunoblotting for pallidin (Fig. 6F).

The sedimentation coefficient and Stokes radius of the HPS1·HPS4 complex were used to calculate its molecular mass and frictional ratio, as described (37). The calculated molecular mass of the complex is ~175 kDa, which approximates the sum of the molecular masses of the HPS1 and HPS4 polypeptides. The frictional ratio of ~1.8 indicates that it is a moderately asymmetric complex.

Yeast Two-hybrid Analysis of the HPS1·HPS4 Interaction—To examine whether the interaction between HPS1 and

HPS4 proteins is direct, we performed yeast two-hybrid analyses (Fig. 7). GAL4bd constructs encoding the full-length HPS1 or HPS4 proteins were co-expressed with GAL4ad constructs encoding the same proteins. There was no evidence of interaction of HPS1 with HPS4, or of self-association of these two proteins (Fig. 7A), despite expression of all of these proteins, as demonstrated by immunoblotting of the co-transformed yeast cells (Fig. 7B).

Trafficking of Lysosomal Membrane Proteins in HPS4-deficient Cells—Defects in the AP-3 complex in fibroblasts and B-lymphoblastoid cells from β 3A-deficient HPS2 patients (6), and in fibroblasts from the β 3A-deficient (6, 22) and δ -deficient mice (6) result in enhanced trafficking of lysosomal membrane proteins such as CD63 and Lamp-1 via the cell surface. Nevertheless, these lysosomal proteins still reach the lysosomes following an endocytic route (6, 39). To determine whether the HPS1·HPS4 complex might be similarly involved in the trafficking of lysosomal membrane proteins, we compared the uptake of antibodies to Lamp-2 and Lamp-1, and the steady-state distribution of these proteins, in primary cultures of wild-type, *pearl* (β 3A-deficient), *pallid* (BLOC-1), *ruby eye* (BLOC-2), and *light ear* (HPS4-deficient) fibroblasts. We observed that wild-type, *pallid*, and *ruby eye* fibroblasts took up barely detectable amounts of anti-Lamp-2 (Fig. 8, A, C, and D) antibody, whereas *pearl* cells internalized noticeable higher amounts (Fig. 8B). Using this assay, *light ear* cells exhibited a pattern of internalization similar to that of the wild-type cells (Fig. 8E). The steady state distributions of Lamp-2 in the cells from all five mice were not detectably different (data not shown). Similar results were observed when the internalization of Lamp-1 antibody and the steady state distributions of Lamp-1 were studied (data not shown). Together with previous findings (29), these observations indicate that, unlike AP-3, the HPS1·HPS4 complex as well as BLOC-1 and BLOC-2 are not directly involved in the trafficking of lysosomal membrane proteins.

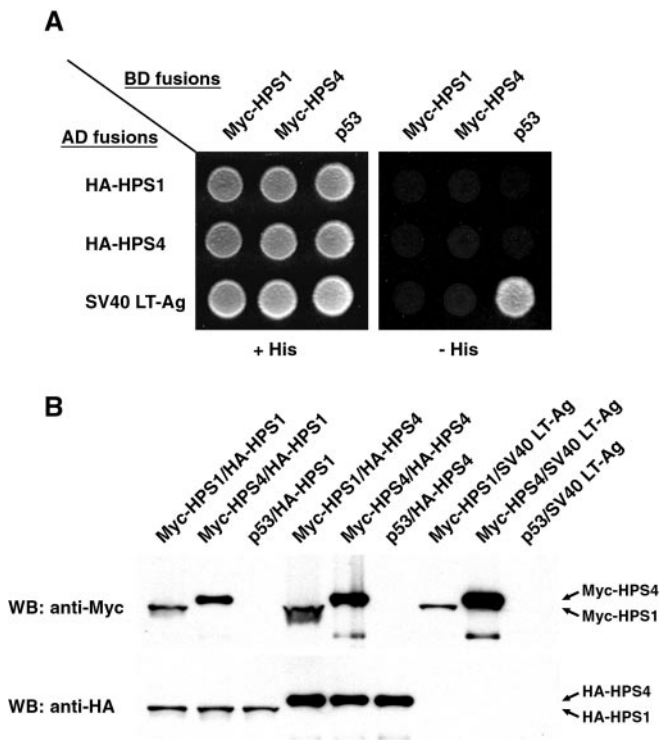


FIG. 7. Yeast two-hybrid analysis of HPS1 and HPS4 interaction. The AH109 yeast strain was co-transformed with full-length *HPS1* and *HPS4* cDNAs fused to GAL4 DNA-binding domain (GAL4bd) and GAL4 transcription activation domain (GAL4ad), respectively, and vice versa. *A*, after selection, co-transformants were plated on plates with (+ *His*) or without (– *His*) histidine. Interactions were detected based on the ability of the co-transformants to grow in the absence of histidine. *B*, whole extracts of the co-transformed yeast cells were subjected to SDS-PAGE and immunoblotting analysis using mouse monoclonal anti-Myc and anti-HA antibodies. Notice that the yeast two-hybrid control proteins (p53 and SV40 LT-Ag) are not fused to epitope tags.

Vesicular Storage of Zinc Ions in HPS4-deficient Cells—Another phenotype associated with AP-3 deficiency in mice is a decrease in vesicular pools of Zn^{2+} (22, 27), which is probably caused by mislocalization or degradation of Zn^{2+} transporters such as ZnT-3 (14). Vesicular Zn^{2+} can be visualized by staining with the membrane-permeant Zn^{2+} fluorescent probe, zinquin (40). Zinquin staining of fibroblasts from *pearl* mice revealed decreased accumulation of Zn^{2+} (Fig. 9B), as previously reported (27). Fibroblasts from *light ear* (HPS4-deficient) mice, as well as those from *pallid* (BLOC-1) and *ruby eye* (BLOC-2) mice, displayed apparently normal zinquin staining (Fig. 9E). Therefore, vesicular storage of Zn^{2+} in fibroblasts is also unaffected by the lack of expression of HPS4. This observation adds to the notion that AP-3 on one side and the HPS1·HPS4, BLOC-1, and BLOC-2 complexes on the other side act at different steps in the biogenesis of LROs.

DISCUSSION

The evidence presented here indicates that the HPS1 and HPS4 proteins are part of a novel complex that, in keeping with the nomenclature in the field, we propose to name BLOC-3 (for biogenesis of lysosome-related organelles complex 3). The molecular mass of this complex, calculated from sedimentation velocity and gel filtration analyses, is ~175 kDa. This corresponds approximately to the sum of the molecular masses of the HPS1 and HPS4 polypeptides, indicating that BLOC-3 has one copy of each of these polypeptides. Yeast two-hybrid assays have failed to demonstrate an interaction of HPS1 and HPS4 expressed as chimeras with the Gal4 DNA binding domain and

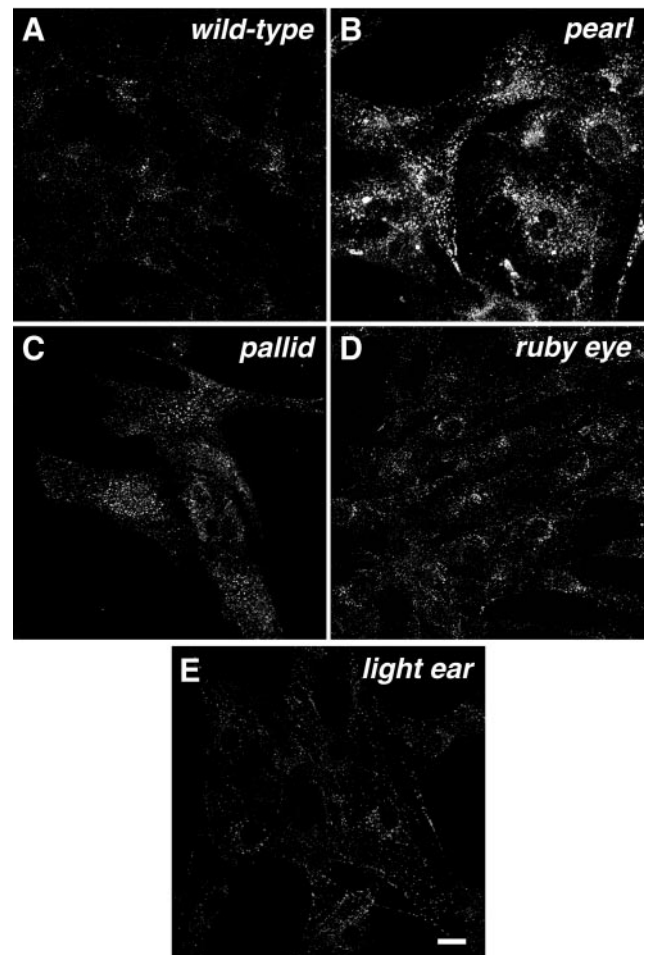


FIG. 8. Trafficking of Lamp-2 via the surface of fibroblasts from wild-type and mutant mice. Skin fibroblasts derived from wild-type (A), *pearl* (B), *pallid* (C), *ruby eye* (D), and *light ear* (E) mice were grown on glass coverslips and then allowed to internalize a rat monoclonal antibody to mouse Lamp-2 for 15 min at 37 °C. Subsequently, cells were washed, fixed in 4% formaldehyde, permeabilized, and processed for immunofluorescence. Bar, 20 μ m.

transcription activation domain, respectively, even though the chimeras are well expressed in the co-transformed yeast cells. A trivial explanation could be that the chimeras expressed in yeast do not behave like the endogenous or epitope-tagged proteins do in mammalian cells. Alternatively, these results could point to the existence of a third component of the BLOC-3 complex, which allows the transgenic HPS1 and HPS4 proteins to come together when expressed by transfection into mammalian cells. This component would have to be very small, however, to fit within the margin of error in the estimation of the size of the BLOC-3 complex.

The physical association of the HPS1 and HPS4 proteins explains the absence of the HPS1 protein from *light ear* (HPS4-deficient) fibroblasts, as unassembled subunits of multiprotein complexes are most often degraded (41). This has also been observed for the unassembled subunits of the AP-3 complex (6, 31) and BLOC-1 (19, 27, 28) in other forms of HPS. The assembly of HPS1 with HPS4 is also consistent with the similar phenotype observed in *pale ear* (HPS1-deficient), *light ear* (HPS4-deficient), and double-homozygote *pale ear/light ear* mice (8, 32).

Subcellular fractionation analyses revealed that BLOC-3 is mostly cytosolic, with only a very small fraction associated with membranes. This could be because of dissociation from membranes during cell lysis. However, we have also observed a

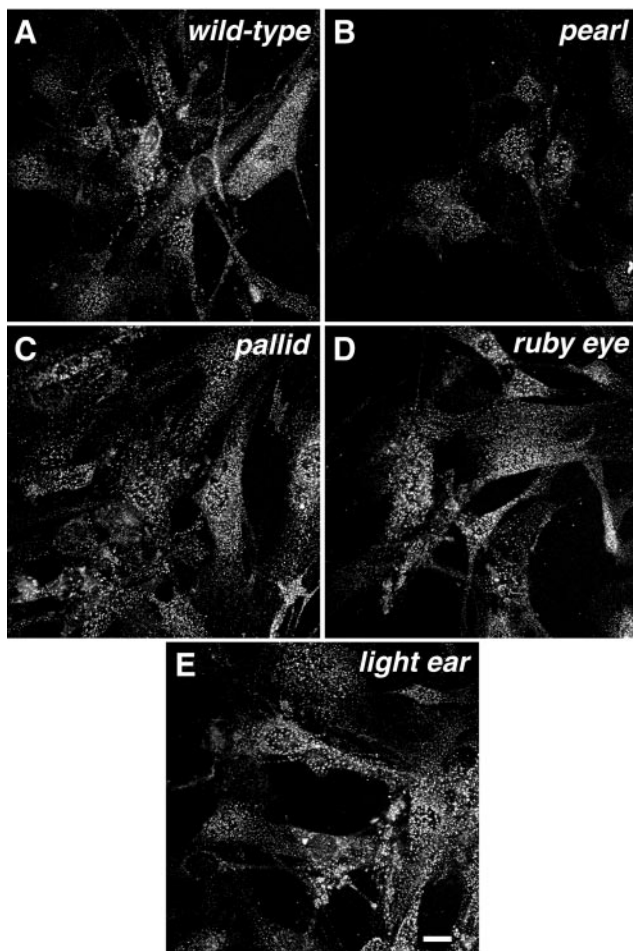


FIG. 9. Intracellular zinc distribution in fibroblasts from wild-type and mutant mice. Skin fibroblasts from wild-type (A), *pearl* (B), *pallid* (C), *ruby eye* (D), and *light ear* (E) mice were grown on monolayers, fixed with formaldehyde, and then incubated with the membrane-permeant fluorescent indicator, zinquin. Images were acquired on a Zeiss LSM 410 confocal microscope using a 413-nm laser. Notice the punctate pattern of zinc-bound zinquin fluorescence (A, C, D and E) that is less defined in B. Bar, 20 μ m.

mostly cytosolic pattern of localization by immunofluorescence microscopy of cells stably expressing both HA₃-HPS1 and Myc₃-HPS4 and we were unable to detect any HPS1·HPS4 complex associated to membranes in cells permeabilized prior to fixation (data not shown). In this regard, BLOC-3 also resembles BLOC-1, which is mostly localized to the cytosol (27, 28). Because both complexes contribute to the biogenesis of membrane-bound organelles, it is likely that the small fraction that is associated with membranes represents the active form of each complex. Studies by Spritz and colleagues (30) have shown that the membrane-associated form of HPS1 localizes to tubulovesicular and pre-melanosomal structures in melanotic cells. Morphological analyses of skin melanocytes from *light ear* (HPS4-deficient) mice have revealed an increase in the proportion of immature melanosomes, which is probably because of a kinetic block in their maturation (42). A reduced number of mature melanosomes and aberrant melanosomes were also observed in retinal pigmented epithelial cells of *light ear* (HPS4-deficient) mice (8). Thus, it is likely that BLOC-3 functions at an early stage of melanosome biogenesis.

The exact biochemical pathway in which BLOC-3 is involved is unknown and, unfortunately, the sequences of both the HPS1 and HPS4 proteins are not informative in this regard. Orthologs of these proteins exist in all mammals with sequenced genomes, as well as in *Drosophila*, but not in the

yeasts *S. cerevisiae* and *Schizosaccharomyces pombe*. This correlates with the existence of LROs in metazoans but not in yeasts. It is likely that, like BLOC-1 and BLOC-2, BLOC-3 is part of the molecular machinery specifically dedicated to LRO biogenesis. In contrast, AP-3 (35, 43, 44) and HOPS/Vps-C (25, 26) exist in all eukaryotes including yeast, exhibit homologies to other proteins, and have known functions in protein trafficking in the endosomal-lysosomal system. These complexes are probably components of the general endosomal-lysosomal trafficking machinery, and their absence leads to other phenotypic abnormalities in addition to those derived from LRO defects. Indeed, we have observed that AP-3 deficiency in fibroblasts causes enhanced trafficking of both Lamp-1 and Lamp-2 via the plasma membrane, whereas BLOC-3 deficiency does not appreciably affect the trafficking of these proteins. Similarly, AP-3-deficient cells exhibit reduced vesicular accumulation of Zn²⁺, whereas BLOC-3-deficient cells display apparently normal Zn²⁺ accumulation.

The possibility that BLOC-3 might be involved in some aspect of lysosome biogenesis, however, cannot be ruled out. *Light ear* (HPS4-deficient) and *pale ear* (HPS1-deficient) mice have enlarged lysosomes with increased amounts of lysosomal hydrolases in the kidney, and decreased secretion of lysosomal hydrolases into the urine (45). In addition, macrophages from *pale ear* mice exhibit reduced secretion of mature lysosomal hydrolases upon treatment with ammonium chloride (20). It remains to be determined whether the lysosomes that undergo exocytosis in these cell types are true lysosomes or LROs.

The biochemical characterization of proteins that are defective in human and mouse models of HPS is thus beginning to uncover a distinct molecular machinery for LRO biogenesis in which various multiprotein complexes play essential roles. The description of the BLOC-3 complex reported here is another step toward unraveling the nature of this machinery.

Acknowledgments—We thank Xiaolin Zhu for excellent technical assistance and Rafael Mattera for comments on the manuscript.

REFERENCES

- Dell'Angelica, E. C., Mullins, C., Caplan, S., and Bonifacino, J. S. (2000) *FASEB J.* **14**, 1265–1278
- Swank, R. T., Novak, E. K., McGarry, M. P., Rusiniak, M. E., and Feng, L. (1998) *Pigment Cell Res.* **11**, 60–80
- Marks, M. S., and Seabra, M. C. (2001) *Nat. Rev. Mol. Cell. Biol.* **2**, 738–748
- Ward, D. M., Shiflett, S. L., and Kaplan, J. (2002) *Curr. Mol. Med.* **2**, 469–477
- Oh, J., Bailin, T., Fukai, K., Feng, G. H., Ho, L., Mao, J. I., Frenk, E., Tamura, N., and Spritz, R. A. (1996) *Nat. Genet.* **14**, 300–306
- Dell'Angelica, E. C., Shotelersuk, V., Aguilar, R. C., Gahl, W. A., and Bonifacino, J. S. (1999) *Mol. Cell* **3**, 11–21
- Anikster, Y., Huizing, M., White, J., Shevchenko, Y. O., Fitzpatrick, D. L., Touchman, J. W., Compton, J. G., Bale, S. J., Swank, R. T., Gahl, W. A., and Toro, J. R. (2001) *Nat. Genet.* **28**, 376–380
- Suzuki, T., Li, W., Zhang, Q., Karim, A., Novak, E. K., Sviderskaya, E. V., Hill, S. P., Bennett, D. C., Levin, A. V., Nieuwenhuis, H. K., Fong, C. T., Castellan, C., Mitterski, B., Swank, R. T., and Spritz, R. A. (2002) *Nat. Genet.* **30**, 321–324
- Zhang, Q., Zhao, B., Li, W., Oiso, N., Novak, E. K., Rusiniak, M. E., Gautam, R., Chintala, S., O'Brien, E. P., Zhang, Y., Roe, B. A., Elliott, R. W., Eicher, E. M., Liang, P., Kratz, C., Legius, E., Spritz, R. A., O'Sullivan, T. N., Copeland, N. G., Jenkins, N. A., and Swank, R. T. (2003) *Nat. Genet.* **33**, 145–153
- Gardner, J. M., Wildenberg, S. C., Keiper, N. M., Novak, E. K., Rusiniak, M. E., Swank, R. T., Puri, N., Finger, J. N., Hagiwara, N., Lehman, A. L., Gales, T. L., Bayer, M. E., King, R. A., and Brilliant, M. H. (1997) *Proc. Natl. Acad. Sci. U. S. A.* **94**, 9238–9243
- Feng, G. H., Bailin, T., Oh, J., and Spritz, R. A. (1997) *Hum. Mol. Genet.* **6**, 793–797
- Feng, L., Seymour, A. B., Jiang, S., To, A., Peden, A. A., Novak, E. K., Zhen, L., Rusiniak, M. E., Eicher, E. M., Robinson, M. S., Gorin, M. B., and Swank, R. T. (1999) *Hum. Mol. Genet.* **8**, 323–330
- Suzuki, T., Li, W., Zhang, Q., Novak, E. K., Sviderskaya, E. V., Wilson, A., Bennett, D. C., Roe, B. A., Swank, R. T., and Spritz, R. A. (2001) *Genomics* **78**, 30–37
- Kantheti, P., Qiao, X., Diaz, M. E., Peden, A. A., Meyer, G. E., Carskadon, S. L., Kapthamer, D., Sufalko, D., Robinson, M. S., Noebels, J. L., and Burmeister, M. (1998) *Neuron* **21**, 111–122
- Detter, J. C., Zhang, Q., Mules, E. H., Novak, E. K., Mishra, V. S., Li, W., McMurtrie, E. B., Tchernev, V. T., Wallace, M. R., Seabra, M. C., Swank, R. T., and Kingsmore, S. F. (2000) *Proc. Natl. Acad. Sci. U. S. A.* **97**,

- 4144–4149
16. Suzuki, T., Oiso, N., Gautam, R., Novak, E. K., Panthier, J. J., Suprabha, P. G., Vida, T., Swank, R. T., and Spritz, R. A. (2003) *Proc. Natl. Acad. Sci. U. S. A.* **100**, 1146–1150
 17. Huang, L., Kuo, Y.-M., and Gitschier, J. (1999) *Nat. Genet.* **23**, 329–332
 18. Zhang, Q., Li, W., Novak, E. K., Karim, A., Mishra, V. S., Kingsmore, S. F., Roe, B. A., Suzuki, T., and Swank, R. T. (2002) *Hum. Mol. Genet.* **11**, 697–706
 19. Ciciotte, S. L., Gwynn, B., Moriyama, K., Huizing, M., Gahl, W. A., Bonifacino, J. S., and Peters, L. L. (2003) *Blood* **101**, 4402–4407
 20. Brown, J. A., Novak, E. K., and Swank, R. T. (1985) *J. Cell Biol.* **100**, 1894–1904
 21. Höning, S., Sandoval, I. V., and von Figura, K. (1998) *EMBO J.* **17**, 1304–1314
 22. Yang, W., Li, C., Ward, D. M., Kaplan, J., and Mansour, S. L. (2000) *J. Cell Sci.* **113**, 4077–4086
 23. Huizing, M., Sarangarajan, R., Strovel, E., Zhao, Y., Gahl, W. A., and Boissy, R. E. (2001) *Mol. Biol. Cell* **12**, 2075–2085
 24. Le Borgne, R., Planque, N., Martin, P., Dewitte, F., Saule, S., and Hoflack, B. (2001) *J. Cell Sci.* **114**, 2831–2841
 25. Seals, D. F., Eitzen, G., Margolis, N., Wickner, W. T., and Price, A. (2000) *Proc. Natl. Acad. Sci. U. S. A.* **97**, 9402–9407
 26. Sato, T. K., Rehling, P., Peterson, M. R., and Emr, S. D. (2000) *Mol. Cell* **6**, 661–671
 27. Falcon-Perez, J. M., Starcevic, M., Gautam, R., and Dell'Angelica, E. C. (2002) *J. Biol. Chem.* **277**, 28191–28199
 28. Moriyama, K., and Bonifacino, J. S. (2002) *Traffic* **3**, 667–677
 29. Dell'Angelica, E. C., Aguilar, R. C., Wolins, N., Hazelwood, S., Gahl, W. A., and Bonifacino, J. S. (2000) *J. Biol. Chem.* **275**, 1300–1308
 30. Oh, J., Liu, Z. X., Feng, G. H., Raposo, G., and Spritz, R. A. (2000) *Hum. Mol. Genet.* **9**, 375–385
 31. Zhen, L., Jiang, S., Feng, L., Bright, N. A., Peden, A. A., Seymour, A. B., Novak, E. K., Elliott, R., Gorin, M. B., Robinson, M. S., and Swank, R. T. (1999) *Blood* **94**, 146–155
 32. Meisler, M. H., Wanner, L., and Strahler, J. (1984) *J. Hered.* **75**, 103–106
 33. Le Borgne, R., Alconada, A., Bauer, U., and Hoflack, B. (1998) *J. Biol. Chem.* **273**, 29451–29461
 34. Dell'Angelica, E. C., Ooi, C. E., and Bonifacino, J. S. (1997) *J. Biol. Chem.* **272**, 15078–15084
 35. Dell'Angelica, E. C., Ohno, H., Ooi, C. E., Rabinovich, E., Roche, K. W., and Bonifacino, J. S. (1997) *EMBO J.* **15**, 917–928
 36. Martina, J. A., Bonangelino, C. J., Aguilar, R. C., and Bonifacino, J. S. (2001) *J. Cell Biol.* **135**, 1111–1120
 37. Marks, M. S. (1998) in *Current Protocols in Cell Biology* (Bonifacino, J. S., Dasso, M., Harford, J. B., Lippincott-Schwartz, J., and Yamada, K., eds) pp. 5.3.1–5.3.33, John Wiley & Sons, New York
 38. Bonifacino, J. S., and Dell'Angelica, E. C. (1998) in *Current Protocols in Cell Biology* (Bonifacino, J. S., Dasso, M., Harford, J. B., Lippincott-Schwartz, J., and Yamada, K., eds) pp. 7.2.1–7.2.21, John Wiley & Sons, New York
 39. Reusch, U., Bernhard, O., Koszinowski, U., and Schu, P. (2002) *Traffic* **3**, 752–761
 40. Zalewski, P. D., Forbes, I. J., and Betts, W. H. (1993) *Biochem. J.* **296**, 403–408
 41. Klausner, R. D., Lippincott-Schwartz, J., and Bonifacino, J. S. (1990) *Annu. Rev. Cell Biol.* **6**, 403–431
 42. Nguyen, T., Novak, E. K., Kermani, M., Fluhr, J., Peters, L. L., Swank, R. T., and Wei, M. L. (2002) *J. Invest. Dermatol.* **119**, 1156–1164
 43. Simpson, F., Peden, A. A., Christopoulou, L., and Robinson, M. S. (1997) *J. Cell Biol.* **137**, 835–845
 44. Cowles, C. R., Odorizzi, G., Payne, G. S., and Emr, S. D. (1997) *Cell* **91**, 109–118
 45. Meisler, M., Levy, J., Sansone, F., and Gordon, M. (1980) *Am. J. Pathol.* **101**, 581–593